

**Identification of Bevacizumab Resistance  
Molecular Signature in Glioblastoma  
by Translating Ribosome Affinity  
Purification (TRAP)**

**A Thesis Submitted to  
the Department of Cancer Biomedical Science  
in Partial Fulfillment of the Requirements  
for the Master's Degree of Science**

**Sreynet Srun**

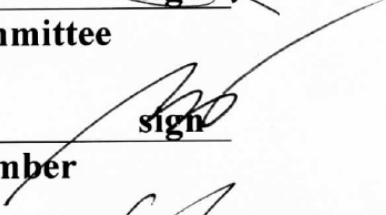
**July 2018**

**National Cancer Center  
Graduate School of Cancer Science and Policy**

**Professor Jong Bae Park**

**We hereby approve the M.S. thesis of  
Sreynet Srun.**

**July 2018**

<b>Gwak, Ho Shin</b>	
_____	sign ✓
<b>Chairman of Thesis Committee</b>	
<b>Park, Jong Bae</b>	
_____	sign
<b>Thesis Committee Member</b>	
<b>Yoo, Byong Chul</b>	
_____	sign
<b>Thesis Committee Member</b>	

**NATIONAL CANCER CENTER  
GRADUATE SCHOOL OF CANCER SCIENCE AND POLICY**

# **ABSTRACT**

## **Identification of Bevacizumab Resistance Molecular Signatures in Glioblastoma by Translating Ribosome Affinity Purification (TRAP)**

Glioblastoma multiforme (GBM) is the most aggressive malignant primary brain tumor with a median overall survival of 14-17 months. Since GBM patients were highly resistant to conventional therapy, Bevacizumab, the most well-known anti-angiogenesis drug, was approved for recurrent GBM treatment. However, Bevacizumab only had improved progression-free survival but not overall survival. Several researches had reported that anti-angiogenesis therapy increased hypoxic tumor microenvironment which may promote cancer cell invasion and metastasis. However, the mechanism of the anti-angiogenesis therapy regulated hypoxia has not been well elucidated. In this study, by using Translational Ribosome Affinity Purification technology (TRAP) and Hypoxia-responsive vector in Bevacizumab treated mice, we identified the four genes namely ANXA1, STMN1, PTTG, and PRDX1 were up-regulation after Bevacizumab treatment. These genes have highly correlated to hypoxic tumor microenvironment, promoted cell migration and associated

with poor survival in GBM; thus might become potential candidates in the development of new therapies to target hypoxic tumor cell and overcome anti-angiogenesis resistance for GBM.

Copyright by

Sreynet Srun

2018

# Contents

<b>1. Introduction.....</b>	<b>1</b>
1.1. Glioblastoma Multiforme (GBM) .....	1
1.2. Bevacizumab (Avastin) .....	2
1.3. Hypoxia .....	3
1.3.1. Tumor Hypoxia .....	3
1.3.2. Hypoxia Inducible Factors (HIFs) .....	4
1.4. Hypoxia-Responsive vector .....	6
1.5. Translating Ribosome Affinity Purification (TRAP) .....	9
<b>2. Study Objectives.....</b>	<b>9</b>
<b>3. Method and Material.....</b>	<b>10</b>
3.1. Cell culture and condition .....	10
3.2. Transfection and Infection .....	11
3.3. Western Blotting .....	12
3.4. Translating Ribosome Affinity Purification (TRAP) .....	12
3.5. Reverse Transcription Polymerase Chain Reaction (RT-PCR) .....	14
3.6. Animals model .....	15
3.7. Immunohistochemistry staining (IHCs) .....	16

3.8. RNA Sequencing and Bioinformatics analysis .....	16
3.9. Statistical analysis .....	17
<b>4. Results .....</b>	<b>17</b>
4.1. Oxygen-dependence of a hypoxia-responsive vector with 5HRE in different glioblastoma cell lines .....	17
4.2. Detection of HIF-1 $\alpha$ protein level after hypoxia exposure .....	20
4.3. Total mRNA and translational mRNA expression correlate with hypoxia-responsive vector .....	22
4.4. Bevacizumab treatment induce hypoxic tumor microenvironment in the xenograft model .....	23
4.5. Bevacizumab treatment induces the up-regulation of ANXA1, STMN1, PTTG1, and PRDX1 .....	25
<b>5. Discussion .....</b>	<b>29</b>
<b>6. Conclusion .....</b>	<b>31</b>
<b>BIBLIOGRAPHY .....</b>	<b>33</b>
<b>ACKNOWLEDGEMENT .....</b>	<b>37</b>

# List of Table

Table 1. Oligonucleotide Primers for pFUGW-HRE-minCMV .....	8
---	---

# List of Figures

Figure 1. Domain structure of HIF- $\alpha$ and HIF- $\beta$ .....	6
Figure 2. Map of lentiviral hypoxia responsive vectors .....	8
Figure3. Diagram of HIF-1 $\alpha$ mediated on transcriptional and translational induced by hypoxia.....	10
Figure 4. Schematic of TRAP method for isolate translation mRNA.....	14
Figure 5. Schematic diagram of the lentiviral hypoxia-responsive vector	19
Figure 6. Validation of lentiviral backbone for gene expression in different GBM cell lines.....	20
Figure7. HIF-1 $\alpha$ protein accumulations in hypoxia condition.....	21
Figure8. The total mRNA and translational mRNA level associate to hypoxia condition .....	23
Figure9. Bevacizumab treatment induce HIF-1 $\alpha$ dependent manner in glioblastoma.....	25
Figure 10. The four up-regulation ANAX1, STMN1, PTTG, and PRDX1 genes induced by Bevacizumab treatment.....	27
Figure11. ANXA1, STMN1, PTTG, and PRDX1 associated with GBM survival from REMBRANDT dataset.....	28

# **1. Introduction**

## **1.1. Glioblastoma Multiforme (GBM)**

Glioblastoma multiforme (GBM) is the grade fourth glioma, classification by World Health Organization (WHO) [1]. It is the most common and aggressive cancerous brain tumor with frequencies of 51.4% of glioma in adults [2, 3]. This disease occurred typically in adult in the age range from 45 to 65 years old and high frequency in men rather than in women with a ratio approximately 1.3:1 [2]. The overall survival is about 12.1 to 14.6 months and only 3 to 5% GBM patients survived longer than 3 years [4]. Pathologists have distinguished GBM from other glioma cancer grades by the necrotic region in the central of the tumor and abnormal microvascular proliferation surround the tumors [1]. The standard treatment for GBM patients is surgical resection followed by radiotherapy and chemotherapy. However, overall survival was only 2.5 months benefited with minimal additional toxicity [5]. Most important, anti-angiogenesis therapy (AAT) was investigated to improve survival and potentially increased progression-free survival 3.4 months, but it had no effects on overall survival [6]. Similarly, an animal model research suggested that the tumor cells responded to AAT initially by decreasing tumor growth; however, they developed resistance and grew robustly [7]. Taking long period treatment by using AAT or Bevacizumab, the tumor would start proliferation and present the necrotic area [8]. Necrosis may result from hypoxia, which is enhanced cell's growth and malignant behavior [9].

## **1.2. Bevacizumab (Avastin)**

Bevacizumab was sold under the brand name Avastin, which is used in many cancer types, such as metastatic colorectal cancer, non-small cell lung cancer, renal cell carcinoma, metastatic breast cancer, ovarian cancer, and prostate cancer [10]. In 2009, Food and Drug Administration (FDA, USA) has approved Bevacizumab injection as an agent for treating recurrent GBM patients [11]. The mechanism of Bevacizumab is a humanized monoclonal IgG<sub>1</sub> antibody (initially it came from the mouse) selective target directed against Vascular Endothelial Growth Factor A (VEGF-A) [12]. VEGF is a well-known cytokine which plays an important role in developing blood vessel in many cancers. Bevacizumab inhibits the interaction between VEGF-A with its receptor, which leads to decrease blood vessel [13]. Recently, in clinical trial phase 3, Bevacizumab was treated for recurrence GBM patients increased progression-free survival, but it had no significant effect on overall survival [6]. Similarly, preclinical data revealed that Bevacizumab treatment caused a decrease of blood vessel but the tumor size not reduced and triggered more hypoxic tumor microenvironment [14]. Studies using mouse xenograft models showed that hypoxia induced by AAT promoted resistant mechanisms, such as vascular mimicry, stromal cell infiltration, and increase tumor cell invasion, which lead to tumor recurrence [15-17]. Regardless of comprehensive research data, the mechanical resistance to Bevacizumab treatment is still not well understood. One possible reason is the difficulty to identify the specific molecular biomarker for

Bevacizumab treatment resistance and cytotoxic in human [18]. Another reason is the resistance to Bevacizumab is depending on physiologic changes during treatment more than genomic alterations [19]. However, new multi-targeted AATs were still failing to improve patient survival and lack a complete understanding of tumor responses to such drugs. Therefore, the study of tumor vascular remodeling and hypoxic tumor microenvironment are necessary to indicate the anti-angiogenic resistance response.

### **1.3. Hypoxia**

#### **1.3.1. Tumor Hypoxia**

Hypoxia is a condition which the body or region of the body is lack of oxygen tension for internal oxygen homeostasis [20]. In 1950, the tumors hypoxia was described by radiation oncologist as conferring resistance to radiotherapy and chemotherapy [21, 22]. The concentrations of oxygen are different due to the tumor types. In normal or soft tumor the oxygen concentration is 3.9% to 9.5%, while it is 1% to 2% in the solid tumor causing by over oxygen using of the intensive proliferation cells and disorganized vasculature surrounds the tumor [3, 23]. Hypoxia plays an important role in the tumor-immune response, the epithelial-mesenchymal transition, metastasis, and enhance tumor angiogenesis [23]. In GBM, under anti-angiogenesis therapy, hypoxia-mediated six mechanisms; invasive and migration; changing cellular metabolism through up-regulating HIF-1 $\alpha$  and involving by Warburg effect; enhance of autophagy; increase of GBM stem cells self-renewal;

GBM-endothelial cell trans-differentiation implications; and vascular formative responses [24]. However, in severe hypoxic condition, tumor cells were proliferated and survived by recruited Akt in mitochondria and phosphorylated pyruvate dehydrogenase kinase 1 (PDK1) on Thr346 to inactivate the pyruvate dehydrogenase complex [25]. Therefore, specific target genes of hypoxic tumors will be an important key to cancer therapeutics.

### **1.3.2. Hypoxia Inducible Factors (HIFs)**

Hypoxia-Inducible Factors (HIFs) are transcription factors that respond to hypoxia [26]. HIF and their downstream genes play as the master regulatory role in both oxygen delivery and adaptation to low-oxygen levels. It has regulated the genes expressed in many cellular processes, including glucose uptake and metabolism, angiogenesis, erythropoiesis, promoting epithelial-to-mesenchymal transition, cell proliferation, apoptosis, and served as a survival factor for cancer cells as well [22, 27, 28]. HIFs consisted two major's subunit, alpha ( $\alpha$ ) and beta ( $\beta$ ) [29]. HIF- $\beta$  is constitutively expressed, whereas HIF- $\alpha$  is induced by hypoxia, both able to make a complex with ARNT, also known as HIF-1 $\beta$  [30] [26]. There are three subunits of the HIF- $\alpha$  (HIF-1 $\alpha$ , HIF-2 $\alpha$ , and HIF-3 $\alpha$ ) and three paralogues of HIF- $\beta$  (Arnt1, Arnt2, and Arnt3) which are the members of the basic-helix-loop-helix-Per-Arnt-Sim (bHLH-PAS) [26]. HIF-2 $\alpha$  is endothelial PAS domain protein 1 (EPAS1) which stabilizes both hypoxia and normoxia condition and it can bind to the aryl hydrocarbon receptor (AHR) nuclear translocator [28].

HIF-1 $\alpha$  is the most well-known member of the HIFs family which involved in the response to hypoxia in many mammalian cells [29]. N-terminal activation domain (N-TAD) and the C-terminal activation domain (C-TAD) are HIF-1 $\alpha$  transactivation domains [31]. HIF-1 $\alpha$  was overexpressed in many cancer types including colon, breast, gastric, lung, skin, ovarian, pancreatic, prostate, renal carcinomas, and glioblastoma. In brain tumors, HIF-1 $\alpha$  immunohistochemistry detected areas of angiogenesis [32, 33]. The recent studies have been demonstrated that HIF-1 $\alpha$  has potential to activate various target genes which involved in an invasion, cell survival, Warburg effect in GBM, and migration by binding to hypoxia-responsive-element (HRE) [34, 35]. In other hands, HIF-1 $\alpha$  has been inducing more aggressive tumor phenotype and associated with resistance to chemotherapy and radiotherapy, however, the mechanisms are still poorly understood [36].

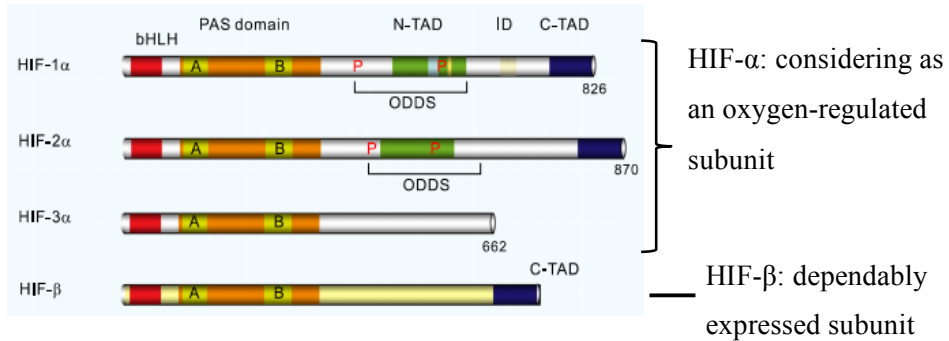


**Figure 1. Domain structure of HIF- $\alpha$  and HIF- $\beta$**

This figure indicates HIF- $\alpha$  isoforms and their co-factor HIF- $\beta$ . HIF- $\beta$  and HIF-2 $\alpha$  are similar, while HIF-3 $\alpha$  seems involved in negative regulation of hypoxia response. Also, this figure represents the structural motifs which are basic Helix-Loop-Helix (bHLH, in red), PER/ARNT/SIM (PAS, in orange), N-terminal transactivation and inhibitory domain (N-TAD and ODDS, in green), C-terminal transactivation (C-TAD, in dark blue). The positions of the protein hydroxylated by prolyl hydroxylase domain containing an enzyme (PDHs) are indicated by P [37].

#### 1.4. Hypoxia-Responsive vector

The role of hypoxia correlates with tumor and cancer positively were mentioned in section 1.3.1. The dominant of HIF-1 $\alpha$  bind to hypoxia-responsive elements (HREs, 5'-ACGTG-3') whereas HRE is one of the oxygen-responsive genes response to hypoxia [38]. HRE is minimal cis-regulatory elements that facilitate transcriptional activation over 60 critical genes of total hypoxia responses [39]. Some of these hypoxia-responsive genes, such as CXCR4 and VEGF, are closely correlated with regulating tumor tropism of NSCs [40]. Therefore, HREs can be resources for transcriptional targeting of tumor hypoxia.

HIF-1 $\alpha$  is up-regulated with 41% among the entire HIF-target gene in a variation of hypoxic microenvironments expression by binding to a cis-acting HRE, however, no all genes, which are transduced by HIF-1 $\alpha$ , can be translated [32] [41]. Thus, the new hypoxia-responsive vector was developed depending on the activation of the hypoxia-selective expression. This vector was constructed by five copies of HREs binding with activated HIF-1 $\alpha$  and following with translational ribosome protein (rpL10a). To increase the hypoxia-inducible level of gene expression, the combination of 5HRE and minimal CMV promoter was constructed and carried out with eGFP reporter gene. The function of this vector was tested by transducing the viral vector to the cancer cells. The transfected cells then were exposed to two difference condition, normoxia and hypoxia, following examined under the fluorescence microscope (Fig1-2) and Table1-1.

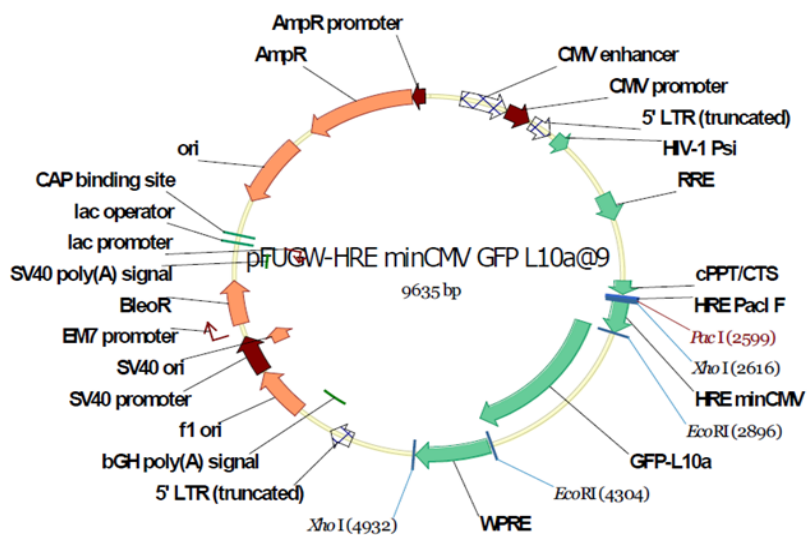


**Figure 2. Map of lentiviral hypoxia responsive vectors**

Lentiviral vectors were respectively incorporated with five copies of the hypoxia-responsive element (HRE) and minimal CMV together work as promoter following with eGFP reporter gene and specific translation ribosome protein (rpL10a).

**Table 1. Oligonucleotide Primers for pFUGW-HRE-minCMV**

#2	pFUGW-HRE_minCMV_GFP_L10a	
Vector	pFUGW-HRE_minCMV	
1st PCR	GFP_ERI_F	agatcactaggaattc gccaccatggtgagcaag
	GFP_L10a_AS	gaaccaccaccagaaccacccttgtagctcgtccatg
	GFP_L10a_S	catggacgagctgtacaag ggtggttctggtggtggttc
	L10a_ERI_r	gcttgatcgaattc ttaatataggcgtgggcttg
	Product size	bp
seq. primer	GFP_ISP	tcttctcaaggacgacg

## **1.5. Translating Ribosome Affinity Purification (TRAP)**

Translating Ribosome Affinity Purification technique (TRAP) is used for specific translation mRNA elution in the cell-type-specific genetic targeting. This technique works both indirect labeling of mRNA and direct cell-type-specific genetic targeting of transgene expression. Indirect labeling of mRNA worked incorporation an affinity label of enhanced Green Fluorescent Protein (eGFP) on the large ribosomal subunit protein L10a (rpL10a). For visualization of the cells transgene, cells were cloned with eGFP-labeled ribosomes. Interestingly, the eGFP-labeled ribosome is not only used as visualization of the cells transgene but also used as an affinity purified labeled ribosomes with the eGFP antibody. In another work, direct cell-type-specific which expression of eGFP-L10a, the cell should engineer with eGFP-L10a and under the direction of the different promoter. Therefore, the purification of cell-type-specific translated mRNA can be eluted if the ribosomes were localized on the mRNA translating upon tissue harvest. The specific translated mRNA that purifies by TRAP can analyze with the downstream technique of TRAP, such as microarray, RNA sequencing, quantitative PCR (qPCR), Northern blot [42].

## **2. Study Objectives**

The aim of this study is to identify the specific molecular signature of HIF-1 $\alpha$  translational gene dependence under anti-angiogenesis therapy. First, we developed the new hypoxia-responsive vector in order to select the translational

gene that correlated with HIF-1 $\alpha$  under hypoxia. By using this vector and TRAP technology, potential candidates would identify.

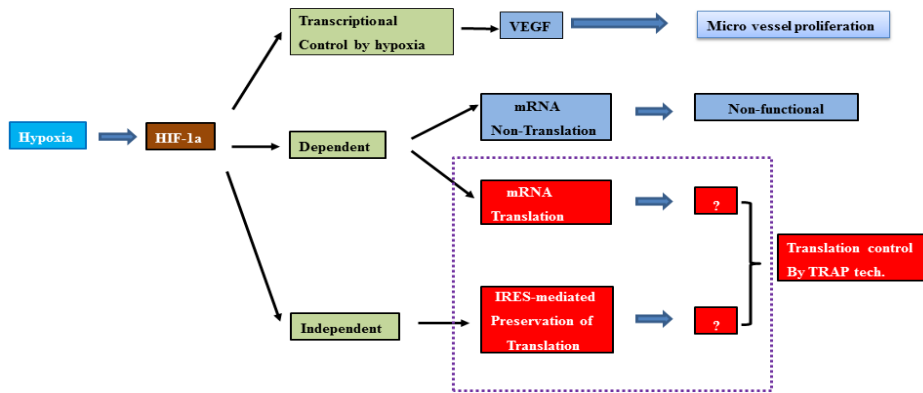


**Figure3. Diagram of HIF-1 $\alpha$  mediated on transcriptional and translational induced by hypoxia**

Under hypoxia condition, transcriptional HIF-1 $\alpha$  genes activate VEGF and induce micro-vessel proliferation. The HIF-1 $\alpha$  gene can be transcribed but not all HIF-1 $\alpha$ -dependent genes can be translated. More important, HIF-1 $\alpha$  upregulates both of translational dependence and independence, two differences results are mRNA and IRES-mediated preservation of translation control. Therefore, the downstream of HIF-1 $\alpha$  gene which results from translate regulation would be found through TRAP technique.

### 3. Method and Material

#### 3.1. Cell culture and condition

U87-MG cells were routinely maintained in a 37 °C humidified atmosphere which containing 5% CO<sub>2</sub> and 95% air in Dulbecco’s Modified Eagle’s Medium High Glucose (DMEM; HyClone), supplemented with 10% Fetal Bovine Serum (FBS; HyClone) and 1% Penicillin (Welgene). Cells were lysed with 0.25%

Trypsin-EDTA (HyClone) for further passage and used for the subsequent study. The cells were cultured in a normoxic condition, 5% CO<sub>2</sub>, 95% air, for 24hrs before exposure to hypoxia condition, 1% O<sub>2</sub>, 5% CO<sub>2</sub>, 94% N<sub>2</sub> (ASTECC, Japan) for, 3hrs, 8hrs, 16hrs, 24hrs, 48hrs, and 72hrs. Cells were reviewing under the fluorescence microscope.

293T cell lines were cultured at 37 °C and 5% CO<sub>2</sub> in DMEM high glucose (HyClone), supplemented with 10% FBS (HyClone), 1% Penicillin (1mM ml<sup>-1</sup>; Gibco by Life Technologies).

### **3.2. Transfection and Infection**

Lentiviruses were generated by co-transfection of vectors with packaging plasmids psPAX2 (Addgene) and pMD2G (Addgene). 293T cells were seeded with a density of 5 x 10<sup>6</sup> cells on 100mm cell culture dishes 24hrs before transfection. Lentiviruses construction are cDNA 5.79µg, psPAX2 4.34µg, and pMD2G 1.45µg were co-transfected into 293T cells using 34.74µl of Lipofectamine<sup>TM</sup> 2000 (Gibco by Life Technologies). The cells were replaced with the medium without antibiotic after 6hrs and incubated for 48hrs at 37 °C and 5% CO<sub>2</sub>. After that, the lentiviruses were harvested and viral particles were concentrated with Lenti-X concentrator (Clontech) with ratio 1:3. These lentiviruses can be used for infection right after the transfection period has done.

For lentiviruses infection, 24hrs prior to infection U87-MG, 83NS, and 528NS cells were seeded into 60mm culture dishes at a density of 5 x 10<sup>5</sup> cells in the 5ml complete medium. Cells were infected with ratio 1:1 of lentiviruses and

medium (medium without antibiotic) under Polybrene (8 $\mu$ g/ml, Sigma-Aldrich) contribution. After 7h30min incubation, medium were changed and cells were incubated for 48hrs. These infected cells were used in next step of our experiment.

### **3.3. Western blotting**

U87-MG naive cell, transgenic cells U87-minCMV-eGFP-hrpL10a, and U87-CMV-eGFP-hrpL10a were seeded at a density of  $1 \times 10^6$  cells and incubated for 24hrs before separated into two groups, normoxic and hypoxic condition. The hypoxia incubation time was 24hrs, 48hrs, and 72hrs. Proteins were extracted with ratio- immunoprecipitation assay buffer (RIPA), the protease inhibitor, and phosphatase inhibitor cocktails (Thermo Scientific). Protein 20 $\mu$ g were separated by 4-12% Tris-Glycine Gels electrophoresis, transferred to polyvinylidene difluoride (PVDF) membranes, blocked with 5% skim milk, and treated with primary antibody for overnight at 4 °C cold room with gentle shaking. The primary antibodies are rabbit anti-HIF-1 $\alpha$  (Bethyl laboratory, BL-124-3F7), rabbit monoclonal anti-eGFP (Abcam, ab184601), and mouse anti- $\beta$ -actin (Santa Cruz). The band visualized by enhanced chemiluminescence (ECL, Miracle<sup>TM</sup>; iNtRON, Biotechnology) and plain film exposure.

### **3.4. Translating Ribosome Affinity Purification (TRAP)**

Mice's brain tissues were removed and perform quickly dissection of desired tissue region and place tissue into ice-cold 1X PBS with dissection buffer (5ml of DMEM F12, 125 $\mu$ l of 1M HEPES-KOH\_pH 7.4, 1.75 $\mu$ l of 1M glucose,

200µl of 1M NaHCO<sub>3</sub>, 50µl of Cycloheximide, and 42.93µl of water) for 30min and washed quickly. The tissue was extracted with lysis buffer (200µl of 1M HEPES KOH \_pH 7.4, 750µl of 2M KCl, 50µl of 1M MgCl<sub>2</sub>, 5µl of 1M DTT, 10µl of Cycloheximide, 100µl of rRNasin, 100µl of Supersasin, 9ml of water, and Roshe protease inhibitors 1T.B). The supernatants were collected and added with NP-40 & DHPC. The anti-eGFP antibody bound to protein L-coated beads on the magnetic and treated to cell-lysate supernatants then incubated with end-over-end rotation for 16-18hrs. Beads were collected on a magnetic rack and immediately placed in the RLT buffer of the RNeasy<sup>R</sup> Mini Kit (QIAGEN). RNA was purified with on-column DNase digestion followed the manufacturer's protocol. The RNA purified in this technique is high enough purity for downstream applications RT-PCR and RNA sequencing.

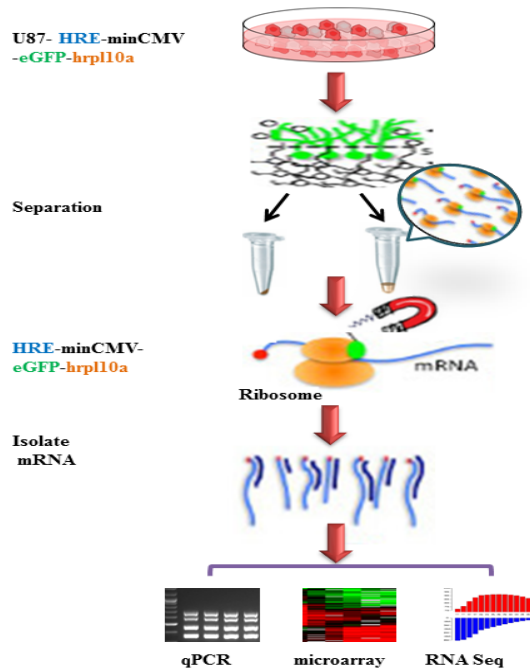


**Figure 4. Schematic of TRAP method for isolate translation mRNA**

U87-MG cell lines were seeded and transfected with a virus encoding an enhancing green fluorescent protein (eGFP) and HRE specifically marker for hypoxia and hrpL10a labels for ribosome mRNA. Later eGFP-hrp110a cells were purified and TRAP method was used to capture ribosome with mRNA bounding. The mRNA yielding was determined by the downstream technique and concludes the protein they encode.

### **3.5. Reverse Transcription Polymerase Chain Reaction (RT-PCR)**

Total RNA and specific translated mRNA from cultured cells were isolated using RNeasy<sup>R</sup> Mini Kit (QIAGEN) and Translating Ribosome Affinity Purification (TRAP) technology, respectively. First-strand complementary cDNA was synthesis using GoScript<sup>TM</sup> M-MLV Reverse Transcriptase system (PROMEGA, Madison WI, USA) with the Random Octamer primers and Oligo

(dT)<sub>36</sub> primer (Gene Link). PCR reaction for each molecule is performed with 94 °C for 5min, 94 °C for 1min and 30sec, 55 °C for 1min, 70 °C for 30sec, 72 °C for 10min, and 4 °C. The total numbers of cycles were performed with 22 cycles of sequential reaction for HIF-1 $\alpha$ , GLUT1, CA9, NDRG1, and B-actin while 21 cycles of VEGF and VEGFA mRNA expression. PCR products were separated by 1% agarose gel electrophoresis and detected under UV light.

### **3.6. Animals model**

Animal studies were conducted in female BALB/c-nude mice and maintained in the animal facility at the National Cancer Center. Tumors were generated with U87-MG naive, U87-HRE-miniCMV-GFP-hrpL10a, and U87-CMV-eGFP-hrpL10a cell by orthotopic xenograft brain injected with 3 $\mu$ l of 5x10<sup>5</sup> cells. Tumors were monitored every once a week by Magnetic Resonant Image (MRI). Beginning three days after injection, the mice were randomized into two groups' Bevacizumab and control (PBS) treatment group. Bevacizumab (Avastin, Genentech, San Francisco) or PBS was intraperitoneally injection administered at 10mg/kg twice weekly in the right and left abdominal for 4 to 6weeks. All the mice brains were collected after 21 to 28days and prepared for other experiments, such as Immunohistochemistry staining (IHC) and mRNA isolation by TRAP. Entirely mice procedures were performed according to the National Cancer Center guidelines for the care and use of laboratory animal. The committee on the Ethics of Animal Experiment (NCC-17-381) approved the protocol.

### **3.7. Immunohistochemistry staining (IHCs)**

Paraffin section samples were used for immunohistochemistry analysis. Mice were anesthetized heart perfusion with cold PBS and fixation with 4% paraformaldehyde (PFA). Paraffin sections, 4 $\mu$ m, were used for histology analysis (immunohistochemistry). The hypoxia imaging on paraffin section was stained with rabbit HIF-1 $\alpha$  antibody (1:100 dilution, monoclonal anti-rabbit, Bethyl laboratory, BL-124-3F7) and incubated in 4  $^{\circ}$ C humidified for overnight. Staining was performed according to the manufacturer's protocol (Pollnk-2 plus HRP Detection Kit/K172713D; GBI Labs).

### **3.8. RNA sequencing and Bioinformatics analysis**

RNA from U87-naive\_control, U87-HRE-minCMV-eGFP-hrpL10a\_Control, and U87-HRE-minCMV-eGFP-hrpL10a\_Avastin treatment groups were used for RNA sequencing. RNA 0.02 ng/ $\mu$ l was used for two rounds of poly (A). The libraries were quantitated using the SMART-Seq v4 Ultra Low Input RNA Kit for sequencing. Using an Illumina HiSeq 2500 to obtain Hundred-nucleotide paired-end reads. Sequencing data was performed on the Theragen Etx Bio Institute server at [www.theragenetex.com/kr/bio](http://www.theragenetex.com/kr/bio). Differential expression analysis was performed using DEG Seq number.

For gene analysis, 8097 genes were obtained after cut-off the genes that have lower than 10 DEG number. Through this analysis, the 40 genes were revealed to be important variables associated with hypoxia respond to AAT.

Next, due to the association between the AAT and hypoxia characteristics of GBM, 20 top up-regulate genes differentially expressed in Bevacizumab treatment and vehicle, ranked by fold change, were significant analysis by using the freely available MeV software (version 4.9.0, [http://mev. tm4.org](http://mev.tm4.org)). This analysis was performed by R and MeV software in all bioinformatics analyses.

### **3.9. Statistical analyzes**

All the data were indicated as the mean  $\pm$  standard deviation ( $\pm$ SD) determined from minimum two independent experiments. Quantitative differences data were analyzed by the two-tailed Student's t-test using Excel software (Microsoft). P-value  $\leq$  0.05 was statistically significant.

## **4. Results**

### **4.1. Oxygen-dependence of a hypoxia-responsive vector with 5HRE in different glioblastoma cell lines**

To understand the mechanism of HIF-1 $\alpha$ -gene-dependence under hypoxia, we developed the hypoxia-responsive vector which has 5HRE and minimal CMV together act as the promoter, followed by specific ribosomal subunit protein L10a (hrpL10a) for translational targeting in glioblastoma. This vector (HRE-miniCMV-eGFP-hrpL10a) was cloned into the pFUGW reporter plasmids and eGFP act as a vector expression (Figure 5A). Another vector which driven by the pFUGW-CMV-eGFP-hrpL10a strong promoter is used as positive control for lentiviral transduction efficiency (Figure 5B). These vectors were co-transfected

into three different glioblastoma cell lines, U87-MG, 83NS, and 528NS. The hypoxia chamber (ASTEC, Japan, 1% O<sub>2</sub>, 5% CO<sub>2</sub>, 94% N<sub>2</sub>) was used for generating the hypoxia condition in vitro confirmed by HIF-1 $\alpha$  immunocytochemistry staining with U87-MG naive cell lines (Figure 6A).

To test vector activities under normoxia (22% O<sub>2</sub>) and hypoxia (1% O<sub>2</sub>) condition, the eGFP level was measured under the fluorescence microscope. Obviously, eGFP was highly expressed in transgenic cells, whereas no eGFP was detected in the cell without gene transfer. In addition, eGFP expression in the hypoxia-responsive promoter (HRE) was displayed negative expression under normoxia whereas highly expressed under hypoxia condition in three groups of glioblastoma cell lines. However, the strong CMV promoter showed no difference between normoxia and hypoxia condition (Figure 6B, C, and D). Thus, HRE-minCMV-eGFP-hrpL10a vector is up-regulated under hypoxia condition in different glioblastoma cell lines.

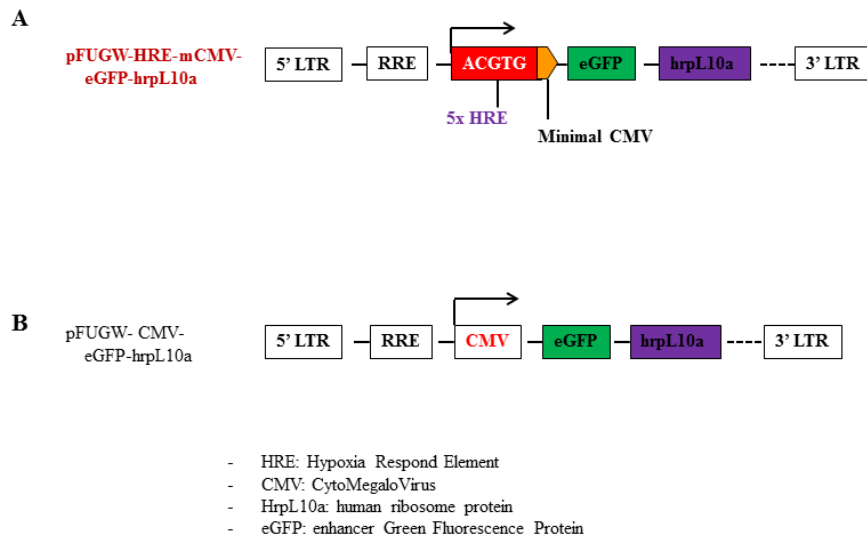


**Figure 5. Schematic diagram of the lentiviral hypoxia-responsive vector**

A) Lentiviral vector was respectively incorporated with five copies of the hypoxia-responsive element (HRE) and minimal CMV together act as the promoter, followed by eGFP visualized gene and specific translation ribosome protein (hrpL10a). B) Lentiviral vector structure of CMV strong promoter is served as positive control for lentiviral transduction efficiency.

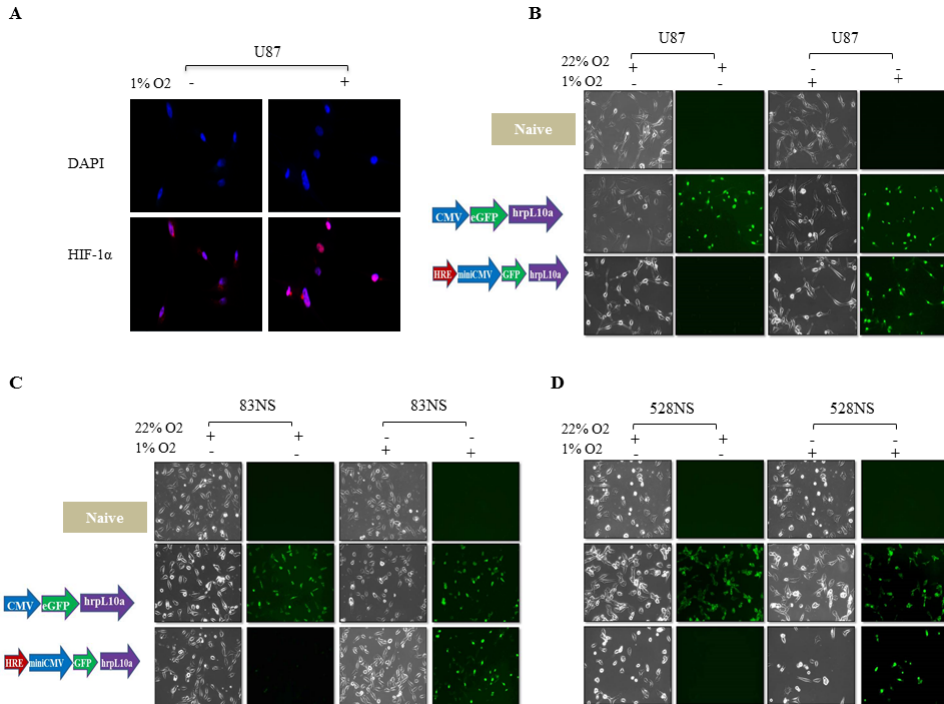


**Figure 6. Validation of lentiviral backbone for gene expression in different GBM cell lines**

A) The U87-MG naive cells were exposed to hypoxia for 24hrs and HIF-1 $\alpha$  was identified by immunocytochemistry. B, C, and D) U87-MG (mesenchymal GBM cell), 83NS (mesenchymal GBM stem cell), and 528NS (proneural GBM stem cell), naive and transgene cells were seeded in two differences conditions normoxia and hypoxia for 24hrs, respectively. The eGFP was observed under the fluorescence microscope.

#### 4.2. Detection of HIF-1 $\alpha$ protein level after hypoxia exposure

To test the achievability of using HRE and minimal CMV promotor for inducing gene expression correlated with intracellular HIF-1 $\alpha$  protein levels under hypoxia, the HIF-1 $\alpha$  protein expression was analyzed in the U87-MG naive and transgenic cells by Western blot. HIF-1 $\alpha$  levels were negatively

expressed under normoxia condition and strongly increased after cell exposed to hypoxia in U87-MG naive and transgenic cell lines (Figure 7B). Interestingly, levels of eGFP proteins were overexpressed in hypoxia condition at 24hrs and it slightly decreased after 72hrs and normoxia in U87-HRE-minCMV-eGFP-hrpL10a (Figure 7A and B). This result suggested that the vector, HRE-minCMV-eGFP-hrpL10a, is dependent on HIF-1 $\alpha$  under hypoxia.

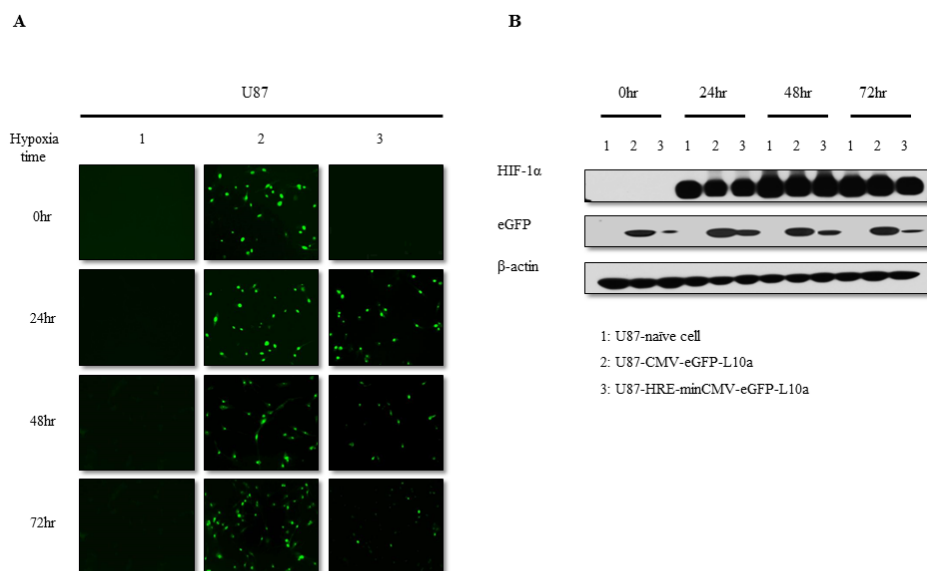


### Figure7. HIF-1 $\alpha$ protein accumulations in hypoxia condition

A) Cells were exposed to hypoxia at 24hr, 48hr, 72hr, and normoxia. The eGFP was observed under the fluorescence microscope. B) Western blot analysis in cell lines with HIF-1 $\alpha$  and eGFP protein at 24hr, 48hr, and 72hrs of hypoxia and normoxia condition. HIF-1 $\alpha$  expression was highly increased following hypoxia condition. The eGFP expression was highly increased following hypoxia at 24hr and 48hr.

HIF-1 $\alpha$ : Hypoxia-Inducible Factor-1 $\alpha$ . eGFP: enhanced Green Fluorescent Protein. 1: U87-MG naive cells. 2: U87MG-CMV-eGFP-hrpL10a. 3: U87MG-HRE-miniCMV-eGFP-hrpL10a.

### **4.3. Total mRNA and translational mRNA expression correlate with hypoxia-responsive vector under hypoxia**

To further demonstrate whether total mRNA and translation mRNAs level are different in hypoxia, the RT-PCR was assessed to examine at mRNA levels of conventional hypoxia markers, HIF-1 $\alpha$ , CA9, GLUT1, NDRG1, VEGF, and VEGFA. Also, the eGFP gene expression level, role as visualizing gene in the transgenic cell line was measured. The result from RT-PCR of total mRNA showed that the hypoxia markers' expression levels were highly expressed after hypoxia at 8hrs and 16hrs, slightly decreased after 3hrs and 24hrs, whereas there was a negative expression in normoxia (Figure 8A). However, the expression of translation mRNA level which extracted by TRAP was highly expressed in hypoxia after 24hrs but negatively expression in normoxia (Figure 8B).

Taken together, these result indicated that our vector, HRE-minCMV-eGFP-hrpL10a, is useful for hypoxia respond in vitro system.

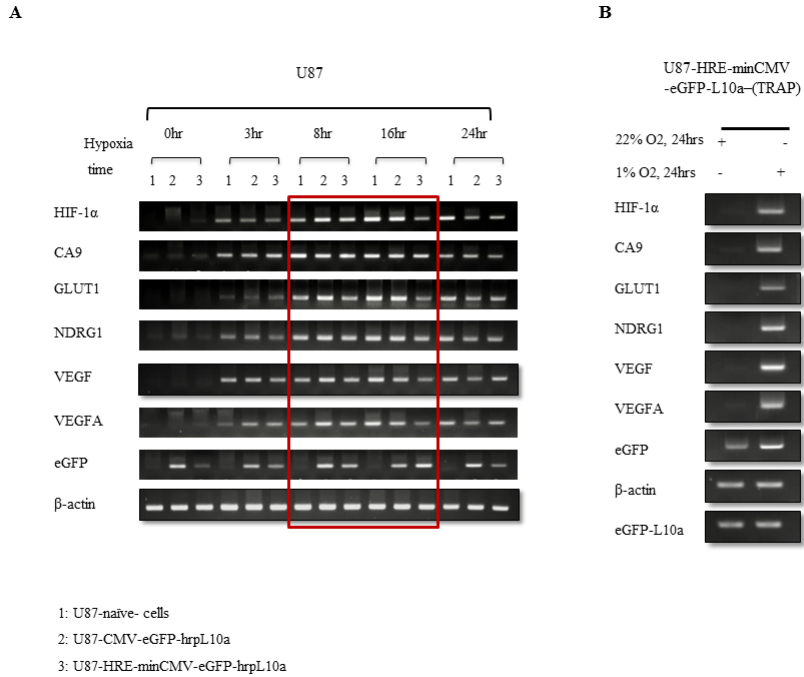


**Figure8. The total mRNA and translational mRNA level associate to hypoxia condition**

A) Detecting the expression of HIF-1 $\alpha$ , CA9, GLUT1, NDRG1, VEGF, VEGFA, and eGFP total mRNA was expressed under hypoxia by RT-PCR, B) and the translation mRNA from TRAP extraction performed by RT-PCR.

#### 4.4. Bevacizumab treatment induce hypoxic tumor microenvironment in the xenograft model

The previous studies suggested that Bevacizumab treatment could induce hypoxia and present necrosis in the tumor core [35]. To understand the effect of anti-VEGF therapy on glioblastoma and determine whether hypoxia vector could apply in vivo under low oxygen tension, animal orthotopic xenograft models were conducted with U87-MG naive cell lines and two transgenic cell lines

groups. After three days of injection, the tumor size was monitored by MRI and started Bevacizumab treatment twice weekly with the dose of 10mg/kg for 4 to 6 weeks (Figure 9A). The entire brain tumors were collected after the tumor implanted and performed immunohistochemistry and mRNA extraction by TRAP technology. In this study, Bevacizumab treatment group has increased the survival period (55days) compare to the vehicle group (43days) with *P-value* =0.0049 (Figure 9B). MRI result showed that the tumor sizes were striking after the first week of treatment and unfortunately, started regrowth rapidly in the third week (Figure 9C). Immunohistochemistry was performed to analyze HIF-1 $\alpha$  expression in tumor sections. The numbers of HIF-1 $\alpha$  positive cells were relatively high in the Bevacizumab treatment group, while they were decreased in the vehicle group (Figure 9D, right). Similarly, in the fresh tissue sections, the endogenous eGFP expression of CMV-eGFP-hrpL10a was not differenced in Bevacizumab treatment and vehicle group, and U87-naive cells line negatively expressed. However, endogenous eGFP expression of HRE-minCMV-eGFP-hrpL10a was strongly expressed in Bevacizumab treatment compared to vehicle group (Figure 9D left). These results demonstrated that Bevacizumab increased the accumulation of transcriptional active HIF-1 $\alpha$  and induced hypoxic tumor microenvironment, which labeled with the eGFP-visualized gene of the hypoxia-responsive vector.

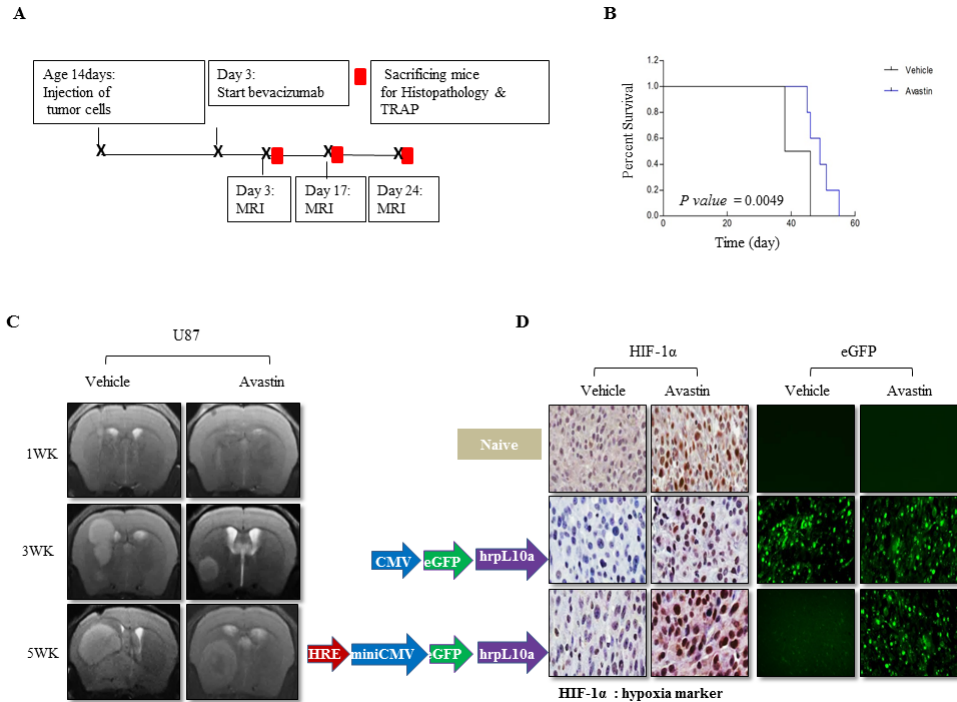


**Figure9. Bevacizumab treatment induce HIF-1 $\alpha$  dependent manner in glioblastoma**

A) Schematic diagram outline the experimental process of anti-angiogenesis orthotopic xenograft mouse model and MRI measurements. B) Kaplan-Meier survival curve of mice bearing Bevacizumab and vehicle treatment ( $P= 0.0049$ ). C) MRI images of the brain in the vehicle and Avastin treatment groups at the first, third and fifth week. D) Immunostaining for HIF-1 $\alpha$  expression in brain tissue section was found in the treatment group but it was not found in the vehicle group (Brown, x200, Fig D right). Fluorescent detection of an endogenous eGFP level of HRE-miniCMV-eGFP-hrpL10a in fresh tissues section was expressed in Bevacizumab treatment group while negatively expressed in the vehicle group (Green, x200, Fig D left).

#### **4.5. Bevacizumab treatment induces the up-regulation of ANXA1, STMN1, PTTG1, and PRDX1**

To confirm the vector system has the ability to label the specific gene under

hypoxia in vivo, RNA profiled were analyzed. Once the treatment period has been finished the mice's brain tissues were removed and perform quickly dissection of desired tissue region where is a high expression of eGFP endogenous (Figure 10A) and mRNAs were immediately extracted by using the TRAP technology. The purity of TRAP result was confirmed with western blot before proceeding RNA sequencing (Figure 10B).

After the RNA sequencing, 15,666genes, 15,225genes, and 13,004genes were obtained in the U87-MG-naive, HRE-minCMV-eGFP-hrpL10a\_vehicle, and HRE-minCMV-eGFP-hrpL10a\_Avastin treatment group, respectively (Figure 10C). Through RNA sequencing and bioinformatics analysis, there were forty genes has been revealed to be important variables associated with hypoxia respond to AAT. Next, due to the association between the AAT and hypoxia characteristics of GBM, the twenty top up-regulate genes differentially expressed in Bevacizumab treatment and vehicle, ranked by fold change, were significant analysis (Figure 10D). When comparing the Bevacizumab treatment and vehicle, the most stable candidate genes for each cell line was B2M, ANXA1, STMN1, PTTG, PRDX1, COX6C, RPL7, and NDUFA. Most important, the four potential candidate genes namely ANXA1, STMN1, PTTG, and PRDX1 have high expression level in Bevacizumab treatment compare to vehicle were identified (Figure 10E). Interestingly, according to Rembrandt-Betastasis dataset was showed those four candidates have high expression in GBM and associate with poor survival also has correlated with HIF-1 $\alpha$  (Figure 11). This suggests that the top four up-regulate are important to investigate the further study.

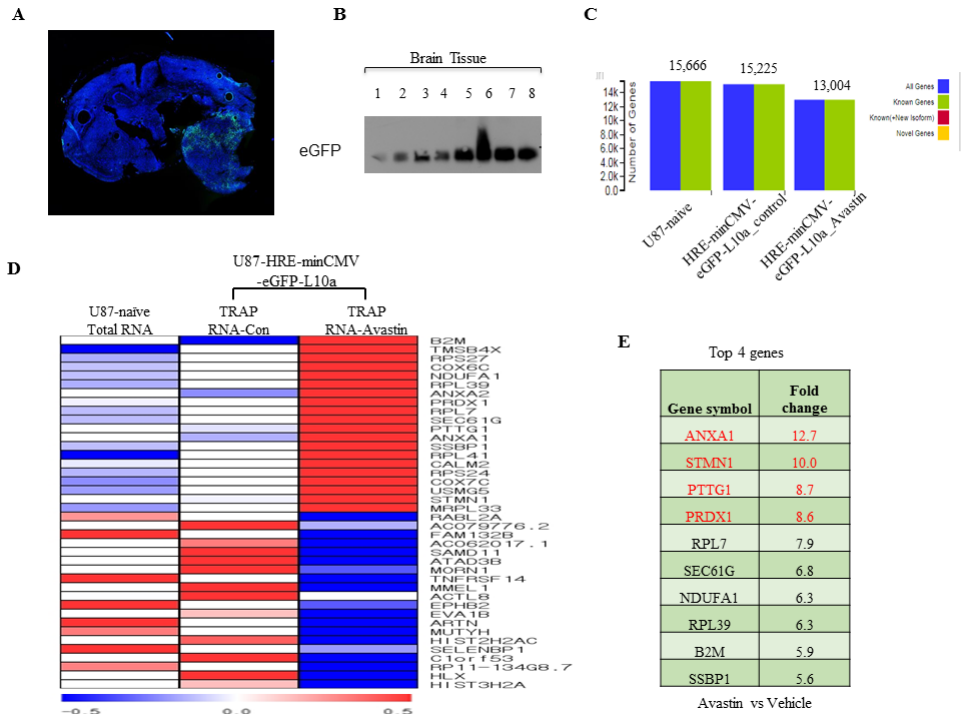


**Figure 10. The four up-regulation ANAX1, STMN1, PTTG, and PRDX1 genes induced by Bevacizumab treatment**

A) The appropriated fresh brain tissue localize with endogenous eGFP expression, which prepares for TRAP experiment. B) The TRAP result confirmation by western blot analyzing the eGFP protein expression level. C) The total genes number of RNA sequence in each group. D) Heat map of 40 most different genes between up-regulation and down-regulation base on DEG number in Bevacizumab treatment and vehicle group, Red indicated high expression, blue indicates low expression, and relative to the average expression of each gene is white, light red, and light blue. E) the top four up-regulate genes expression ranked by fold change.

**Note:** 1. Control brain tissue (unbound fraction) 10ul; 2. Avastin brain tissues (unbound fraction) 10ul; 3. Control brain tissue (unbound fraction) 20ul; 4. Avastin brain tissue (unbound fraction) 20ul; 5. Control brain tissue (bound fraction) 10ul; 6. Avastin brain tissue (bound fraction) 10ul, 7. Control brain tissue (bound fraction) 20ul; 8. Avastin brain tissue (bound fraction) 20ul

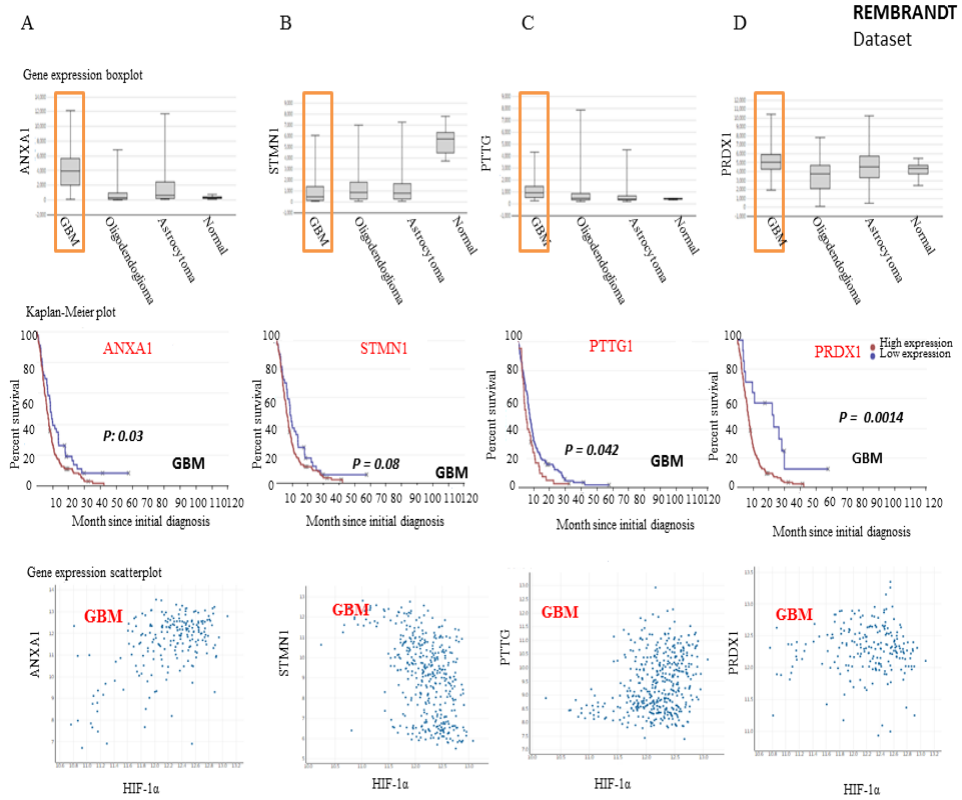


**Figure11. ANXA1, STMN1, PTTG, and PRDX1 associated with GBM survival from REMBRANDT dataset**

A, C, and D) The ANXA1, PTTG, PRDX1 genes expressed highly in GBM compared to normal tissue. ANXA1, PTTG, PRDX1 genes' expression level positive affected by HIF-1 $\alpha$  and associated with poor survival in GBM with *P-value* = 0.03/0.042/0.001, respectively. B) The STMN1 gene expression is lower compared to normal tissue however it poorly survives with *P-value* = 0.08 in GBM and relatively fair with HIF-1 $\alpha$ .

## 5. Discussion

Glioblastoma is the most common primary brain tumor and highly malignant with 15 months survival [3]. Since GBM has enriched the blood vessel and produced a lot of VEGF, anti-angiogenesis therapy (AAT) could be used. However, AAT had affected to increase progression-free survival, but it had no effect on overall survival in patients with recurrence glioblastoma [6]. Tumor cells were resistant to AAT and induced huge necrosis whereas highly hypoxic areas [7, 8]. The underlying mechanisms of this shift require elucidation for therapeutic improvement.

To investigate this phenomenon, the new specific hypoxia-responsive vector was developed. In vitro system, the eGFP signal correlated with heterogeneous HIF-1 $\alpha$  protein levels was found in hypoxia condition only (Figure 6 and 7). This finding led to consider the possibility this vector works as a biomarker for HIF-1 $\alpha$  gene dependent under hypoxia. To further elucidate that vector could be a specific mark for translational gene dependent under hypoxia, the translation mRNAs were isolated by using a specific technique (TRAP), which can only pull down the ribosome mRNA. The result showed that translational mRNA relatively high expression under hypoxia at 24hrs (Figure 8). This finding indicates that the vector is specific for translational hypoxia gene dependent in glioblastoma and the TRAP technology useful in vitro cell lines. To further demonstrate whether this vector could be marked in vivo, the orthotopic xenograft mouse model was generated and treated with Bevacizumab to induce

hypoxia condition through block VEGFA. The data revealed that the endogenous eGFP in fresh tissue section relatively highly expressed in Bevacizumab treatment but it did not express in a vehicle group. Interestingly, the HIF-1 $\alpha$  level was highly expressed in Bevacizumab treatment as well (Figure 9). These results demonstrated that Bevacizumab treatment increased accumulation of transcriptional active HIF-1 $\alpha$  and induced hypoxic tumor microenvironment, which labeled with the eGFP-visualized gene of hypoxia-responsive vector.

To evaluate the benefit of this vector, the translational gene profiles were analyzed. By gene analysis, the 20 top up-regulation genes were strongly expressed in Bevacizumab treatment and associated with hypoxia. Among those 20 candidates, four candidates namely ANXA1, STMN1, PTTG, and PRDX1 were the highest expressed, by fold changing, in Bevacizumab treatment compared to vehicle group (Figure 10). The first candidate, ANXA1, was implicated in maintaining the homeostatic environment within the entire body due to its ability to affect cellular signaling [43]. ANXA1 was indicated as protein membrane which overexpressed in the invasive stages and a key mediator of hypoxia-related in prostate cancer and GBM [44, 45]. ANXA1 was responding to macrophage polarization, promote tumor growth, and decrease survival in vivo [46]. The second candidate, STMN1 was reported to induce migration potential and regulates cell cycle which role in malignant progression of astrocytoma [47]. STMN1 linked to HIF-1 $\alpha$  protein accumulation which involved short survival in breast cancer [47-49]. The third candidate, Pituitary tumor transforming gene (PTTG) was reported as a cell proliferation marker, the overexpression of PTTG

correlates with lymph node infiltration, enhanced cell migration, invasion, and a higher grade of tumor recurrence through activating FAK/Akt/mTOR pathway and contribute to promoting angiogenesis [50-52]. Last candidate, Peroxiredoxin1 (PRDX1) has been demonstrating to play an important role in hypoxia-induced inflammation and cell protection against oxidative stress by detoxifying peroxides and as a sensor of hydrogen peroxide-mediated signaling events [53]. PRDX1 expression was likely to participate in angiogenesis and correlated with hypoxic tumor microenvironment and inflammatory cytokines by regulating the intracellular concentrations of H<sub>2</sub>O<sub>2</sub> [54, 55].

## **6. Conclusion**

Through this study, I could conclude as following: first, the hypoxia-responsive vector was confirming with hypoxia protein markers by western blot after exposure 24, 48, and 72hrs in hypoxia chamber; secondly HRE-minCMV-eGFP-L10a vector was verified under hypoxia condition through observing eGFP expression in different glioblastoma cell lines; thirdly; mRNAs were highly expressed in hypoxia than normoxia condition proved by both Qiagen RNA extraction and TRAP technology. In a word, these result indicated HRE-inCMV-eGFP-L10a vector was a meaningful hypoxia-responsive vector. In addition, the Bevacizumab-treated animal model showed prolongs survival duration and highly accumulation HIF-1 $\alpha$  protein level. Taken together, this hypoxia-responsive vector system would become as a value in both vitro and vivo.

More important, through this study, we found the four potential candidate genes namely, ANXA1, STMN1, PTTG, and PRDX1 highly expressed in the Bevacizumab treatment compared to vehicle and may contribute to Bevacizumab resistant. Further studies about these four genes functions and mechanism should be investigated. We hope that these volunteer candidates will provide a window for increasing survival benefits of the antiangiogenic therapeutics and developing new cancer therapeutic

## BIBLIOGRAPHY

1. Louis, D.N., et al., *The 2007 WHO Classification of Tumours of the Central Nervous System*. Acta Neuropathologica, 2007. **114**(2): p. 97-109.
2. Jawhari, S., M.H. Ratinaud, and M. Verdier, *Glioblastoma, hypoxia and autophagy: a survival-prone 'menage-a-trois'*. Cell Death Dis, 2016. **7**(10): p. e2434.
3. Preusser, M., et al., *Current concepts and management of glioblastoma*. Ann Neurol, 2011. **70**(1): p. 9-21.
4. Krex, D., et al., *Long-term survival with glioblastoma multiforme*. Brain, 2007. **130**(Pt 10): p. 2596-606.
5. Stupp , R., et al., *Radiotherapy plus Concomitant and Adjuvant Temozolomide for Glioblastoma*. New England Journal of Medicine, 2005. **352**(10): p. 987-996.
6. Gilbert , M.R., et al., *A Randomized Trial of Bevacizumab for Newly Diagnosed Glioblastoma*. New England Journal of Medicine, 2014. **370**(8): p. 699-708.
7. Casanovas, O., et al., *Drug resistance by evasion of antiangiogenic targeting of VEGF signaling in late-stage pancreatic islet tumors*. Cancer Cell, 2005. **8**(4): p. 299-309.
8. de Groot, J.F., et al., *Tumor invasion after treatment of glioblastoma with bevacizumab: radiographic and pathologic correlation in humans and mice*. Neuro Oncol, 2010. **12**(3): p. 233-42.
9. Das, S. and P.A. Marsden, *Angiogenesis in Glioblastoma*. The New England journal of medicine, 2013. **369**(16): p. 1561-1563.
10. Mukherji, S.K., *Bevacizumab (Avastin)*. American Journal of Neuroradiology, 2010. **31**(2): p. 235-236.
11. Cohen, M.H., et al., *FDA Drug Approval Summary: Bevacizumab (Avastin®) as Treatment of Recurrent Glioblastoma Multiforme*. The Oncologist, 2012. **17**(11): p. 1482-1482.
12. Fine , H.A., *Bevacizumab in Glioblastoma — Still Much to Learn*. New England Journal of Medicine, 2014. **370**(8): p. 764-765.
13. Tejpar, S., H. Prenen, and M. Mazzone, *Overcoming Resistance to Antiangiogenic Therapies*. The Oncologist, 2012. **17**(8): p. 1039-1050.
14. Keunen, O., et al., *Anti-VEGF treatment reduces blood supply and increases tumor cell invasion in glioblastoma*. Proceedings of the National Academy of Sciences of the United States of America,

2011. **108**(9): p. 3749-3754.
15. van Beijnum, J.R., et al., *The great escape; the hallmarks of resistance to antiangiogenic therapy*. Pharmacol Rev, 2015. **67**(2): p. 441-61.
  16. Welti, J.C., et al., *Fibroblast growth factor 2 regulates endothelial cell sensitivity to sunitinib*. Oncogene, 2011. **30**(10): p. 1183-93.
  17. Selvakumaran, M., et al., *Autophagy inhibition sensitizes colon cancer cells to antiangiogenic and cytotoxic therapy*. Clin Cancer Res, 2013. **19**(11): p. 2995-3007.
  18. Santos, L.V., et al., *VEGF-A levels in bevacizumab-treated breast cancer patients: a systematic review and meta-analysis*. Breast Cancer Res Treat, 2015. **151**(3): p. 481-9.
  19. Missiaen, R., et al., *Targeting endothelial metabolism for anti-angiogenesis therapy: A pharmacological perspective*. Vascul Pharmacol, 2017. **90**: p. 8-18.
  20. Thakor, F.K., et al., *Pharmacological effects of asiatic acid in glioblastoma cells under hypoxia*. Molecular and Cellular Biochemistry, 2017. **430**(1): p. 179-190.
  21. Rankin, E.B. and A.J. Giaccia, *The role of hypoxia-inducible factors in tumorigenesis*. Cell death and differentiation, 2008. **15**(4): p. 678-685.
  22. Rapisarda, A., et al., *Increased antitumor activity of bevacizumab in combination with hypoxia inducible factor-1 inhibition*. Mol Cancer Ther, 2009. **8**(7): p. 1867-77.
  23. LaGory, E.L. and A.J. Giaccia, *The Ever Expanding Role of HIF in Tumour and Stromal Biology*. Nature cell biology, 2016. **18**(4): p. 356-365.
  24. Mahase, S., et al., *Hypoxia-Mediated Mechanisms Associated with Antiangiogenic Treatment Resistance in Glioblastomas*. Am J Pathol, 2017. **187**(5): p. 940-953.
  25. Chae, Y.C., et al., *Mitochondrial Akt Regulation of Hypoxic Tumor Reprogramming*. Cancer Cell, 2016. **30**(2): p. 257-272.
  26. LaGory, E.L. and A.J. Giaccia, *The ever-expanding role of HIF in tumour and stromal biology*. Nat Cell Biol, 2016. **18**(4): p. 356-65.
  27. Qiu, G.Z., et al., *Reprogramming of the Tumor in the Hypoxic Niche: The Emerging Concept and Associated Therapeutic Strategies*. Trends Pharmacol Sci, 2017. **38**(8): p. 669-686.
  28. Rapisarda, A., et al., *Identification of small molecule inhibitors of hypoxia-inducible factor 1 transcriptional activation pathway*. Cancer Res, 2002. **62**(15): p. 4316-24.
  29. Kumar, H. and D.K. Choi, *Hypoxia Inducible Factor Pathway and*

- Physiological Adaptation: A Cell Survival Pathway? Mediators Inflamm*, 2015. **2015**: p. 584758.
30. Zagorska, A. and J. Dulak, *HIF-1: the knowns and unknowns of hypoxia sensing*. *Acta Biochim Pol*, 2004. **51**(3): p. 563-85.
  31. Walsh, J.C., et al., *The Clinical Importance of Assessing Tumor Hypoxia: Relationship of Tumor Hypoxia to Prognosis and Therapeutic Opportunities*. *Antioxidants & Redox Signaling*, 2014. **21**(10): p. 1516-1554.
  32. Zhong, H., et al., *Overexpression of hypoxia-inducible factor 1alpha in common human cancers and their metastases*. *Cancer Res*, 1999. **59**(22): p. 5830-5.
  33. Maynard, M.A. and M. Ohh, *The role of hypoxia-inducible factors in cancer*. *Cell Mol Life Sci*, 2007. **64**(16): p. 2170-80.
  34. Kaur, B., et al., *Hypoxia and the hypoxia-inducible-factor pathway in glioma growth and angiogenesis*. *Neuro Oncol*, 2005. **7**(2): p. 134-53.
  35. Wang, G.L., et al., *Hypoxia-inducible factor 1 is a basic-helix-loop-helix-PAS heterodimer regulated by cellular O2 tension*. *Proceedings of the National Academy of Sciences of the United States of America*, 1995. **92**(12): p. 5510-5514.
  36. Du, R., et al., *HIF1α Induces the Recruitment of Bone Marrow-Derived Vascular Modulatory Cells to Regulate Tumor Angiogenesis and Invasion*. *Cancer cell*, 2008. **13**(3): p. 206-220.
  37. Chen, L., A. Endler, and F. Shibasaki, *Hypoxia and angiogenesis: regulation of hypoxia-inducible factors via novel binding factors*. *Experimental & Molecular Medicine*, 2009. **41**(12): p. 849-857.
  38. Marignol, L., et al., *Achieving hypoxia-inducible gene expression in tumors*. *Cancer Biol Ther*, 2005. **4**(4): p. 359-64.
  39. Semenza, G.L., *Targeting HIF-1 for cancer therapy*. *Nat Rev Cancer*, 2003. **3**(10): p. 721-32.
  40. Zhao, D., et al., *Neural Stem Cell Tropism to Glioma: Critical Role of Tumor Hypoxia*. *Molecular Cancer Research*, 2008. **6**(12): p. 1819.
  41. Benita, Y., et al., *An integrative genomics approach identifies Hypoxia Inducible Factor-1 (HIF-1)-target genes that form the core response to hypoxia*. *Nucleic Acids Research*, 2009. **37**(14): p. 4587-4602.
  42. Heiman, M., et al., *Cell-Type-Specific mRNA Purification by Translating Ribosome Affinity Purification (TRAP)*. *Nature protocols*, 2014. **9**(6): p. 1282-1291.
  43. Sheikh, M.H. and E. Solito, *Annexin A1: Uncovering the Many*

- Talents of an Old Protein*. Int J Mol Sci, 2018. **19**(4).
44. Bizzarro, V., et al., *Hypoxia regulates ANXA1 expression to support prostate cancer cell invasion and aggressiveness*. 2017. **11**(3): p. 247-260.
  45. Mallawaarachy, D.M., et al., *Membrane proteome analysis of glioblastoma cell invasion*. J Neuropathol Exp Neurol, 2015. **74**(5): p. 425-41.
  46. Moraes, L.A., et al., *Annexin-A1 enhances breast cancer growth and migration by promoting alternative macrophage polarization in the tumour microenvironment*. 2017. **7**(1): p. 17925.
  47. Marie, S.K., et al., *Stathmin involvement in the maternal embryonic leucine zipper kinase pathway in glioblastoma*. Proteome Sci, 2016. **14**: p. 6.
  48. Gou, J., et al., *Stathmin 1 plays a role in endometrial decidualisation by regulating hypoxia inducible factor-1alpha and vascular endothelial growth factor during embryo implantation*. Reprod Fertil Dev, 2017. **29**(8): p. 1530-1537.
  49. Obayashi, S., et al., *Stathmin1 expression is associated with aggressive phenotypes and cancer stem cell marker expression in breast cancer patients*. Int J Oncol, 2017. **51**(3): p. 781-790.
  50. Gao, H., et al., *PTTG promotes invasion in human breast cancer cell line by upregulating EMMPRIN via FAK/Akt/mTOR signaling*. Am J Cancer Res, 2016. **6**(2): p. 425-39.
  51. Iliadis, A., et al., *PTTG-1 (Securin) immunoeexpression in meningiomas correlates with tumor grade and proliferation rate: potential use as a diagnostic marker of malignancy*. Apmis, 2018. **126**(4): p. 295-302.
  52. Cristina, C. and G.M. Luque, *Angiogenesis in pituitary adenomas: human studies and new mutant mouse models*. 2014. **2014**: p. 608497.
  53. Cai, C.Y., et al., *Expression and clinical value of peroxiredoxin-1 in patients with pancreatic cancer*. Eur J Surg Oncol, 2015. **41**(2): p. 228-35.
  54. Sun, Q.K., et al., *Diagnostic and prognostic significance of peroxiredoxin 1 expression in human hepatocellular carcinoma*. Med Oncol, 2014. **31**(1): p. 786.
  55. Liu, C.H., et al., *Peroxiredoxin 1 induces inflammatory cytokine response and predicts outcome of cardiogenic shock patients necessitating extracorporeal membrane oxygenation: an observational cohort study and translational approach*. J Transl Med, 2016. **14**(1): p. 114.

# ACKNOWLEDGEMENT

Firstly, I would like to thank my Almighty God for being always with me in all my steps.

I extend my sincere appreciation to my academic advisor Professor Jong Bae Park for his unwavering support and encouragement throughout this entire learning process. His office's door was always opened whenever I ran into trouble spot or had a question related to my study. His generous heart and guidance had steered me in the right direction.

I am grateful to my committees; Professor Ho Shin Gwak and Professor Byong Chul Yoo for their valuable advice and engagement that allowed me to complete this master's thesis.

I would also like to express my deepest gratitude to Mr. Sung Soo Kim who taught me everything in science field from the beginning point. Without his persistent help, this thesis data would not have been possible.

I appreciate to my lab members; Ph.D Jinlong Yin, MD, Ph.D Joon Hee Hong, Mr. Tae Hoon Kim, PhD Young Tae Oh, Ms. Tran Thi Anh Tho, Ms. Wei Wei Lin, Ms. Eun Ji Chor, Mr. Saewhan Park, Mr. Hyung Joon Kwon, and Ms. Yeoun Hee You who support me during experiment difficulties.

In addition, I would sincerely thank Professor SunBook Chang, MD, Ph.D. In-Soo Suh, MD Young Woo Kang, Mr. Jong Cheol Kim, Ms. Lee Jong Sook, and Logo English Ministry church members for their financial and emotional support during this study.

Finally, I must express my very profound gratitude to my family for their metal support and continuous encouragement throughout my years of study even though they were in my home Country-Cambodia.

This accomplishment would not have been possible without them. Thank you!